Insole customized Part 2: 2D/3D graphical process

Maneesh Kumar Mishra[1, 2, 3], Pascal Bruniaux[1, 2, 3], Guillaume Tartare[1, 2, 3] and Christine Campagne[1, 2, 3]

[1] University of Lille Nord de France, Lille, France

[2] Ecole Nationale Supérieure des Arts et Industries Textiles, Roubaix, France

[3]GEMTEX, Roubaix, France

E-mail: Maneesh09mishra@gmail.com, maneesh.mishra@ensait.fr

Original scientific paper

UDK: [685.34.02.073:615.477]:[685.34.017:004.925.84]

DOI: 10.34187/ko.68.3.5

Abstract:

The needs in the sector of orthopedic insoles are becoming more important. The medical purpose of these plantar prostheses is often to correct the posture or biomechanical imbalance that tends to cause pain in various areas of the body depending on the pathology of the patient. This is due to the progression of people who are increasingly obese or have problems with diabetes or other diseases. But, the cost of its products can vary from one to two or more depending on the quality of the product that requires adaptation by a manual process to the morphology of the foot. Whatever the therapeutic product envisaged, the economic model is no longer adapted to the needs of patients and the budgetary imperatives of social security. A new creative process is needed and must incorporate digital tools to reduce these manufacturing costs while improving the quality of products. This study is the continuity of previous works. The process that was used to detect the anthropometric points of the foot was incorporated into a process of creating customized insoles. By combining the technique that extracts the outline encompassing the footprint, a specific process that uses this outline to create the 2D shape of the insole and the using of 3D shape of the standard shoe-last, we have created the 3D shape of the insole adjusted to foot.

Keywords:

3D graphical process, 3D insole model, foot morphology, foot anthropometry, customized insole.

1. Introduction

Previous work has been to take stock of the means of measurement used and analyze the profession of podiatrists by highlighting the medical and economic aspects to detect the technological barrier [1][2][3][4][5][6]. The implementation of a new design process for these therapeutic foot products required the acquisition of morphological, anthropometric and biomechanical knowledge of the foot. In order to characterize the foot dimensionally and morphologically, a process of detection of anthropometric points and the creation of morphological curves has been implemented (part one of this work).

The needs in the sector of orthopedic insoles are becoming stronger. The medical purpose of these plantar prostheses is to correct the posture or biomechanical imbalance that tends to cause pain in various areas of the body depending on the pathology of the patient [7][8][9][10]. The therapeutic indications that are most often recommended are found in the case of osteoarthritis pain of the knee or hip, legs, unequal length, cavus or planus feet or hyper pressure zones [11][12]. These pathologies are usually detected by rheumatologists or podiatrists. The latter finalize the prescriptions by the manufacture of custom-made orthopedic insoles that will be worn for about a year (normal life of the orthopedic insoles). These pathologies can be found in particular in children, athletes, disabled and elderly people [13][1][14] . Depending on the practitioner, the cost can vary from single to double or more (75€ to 300€) depending on the quality of the insole and the prescription since the manufacturing techniques are very traditional. In addition, the ceiling for social security reimbursements is not very high and does not take into account the inherent purchase of specific shoes in pharmacy to integrate this additional volume.

Whatever the therapeutic product envisaged, the economic model is no longer adapted to the needs of patients and the budgetary imperatives of social security. It must be based on the reflection of a coherent value chain to adjust a relevant response to needs by integrating the operating model of podiatrists or medical doctors and their level of acceptance to change, to define the right value chain. Of course, setting up a digital design process for these different products can only help to improve them while reducing production costs.

To replace the old process [15], the implementation of a new process for the design of therapeutic products for the feet will require the feet's knowledge on different aspects. The morphology of the foot is very useful in the creation of the shoe because it depends on the shoe-last. In the same way, The morphology of the shoe-last is very useful in the creation of the insole [16] .

Anthropometry is the means of measuring the foot to characterize it dimensionally [17]. But, from one patient to another, with the same size, some dimensions can be very different, which can be problematic. On the biomechanical aspect, the foot's pressure on the insole must be correct because it can cause various disorders or pain mentioned above.

This morphological and anthropometric knowledge of the foot will require the implementation of a reliable 3D digital measurement process. For this, we must detect the anthropometric points allowing precise measurements by a specific process [18]. Thus, they will not depend on the anthropometric rules or the position of markers placed manually on the foot such as those used by a 3D scanner (industrial measurements) [19].

A customized orthopedic insole must be studied to understand how it is located between the foot and the bottom of the shoe. The upper part of the orthopedic insole is supposed to represent the lower surface of the foot in order to correctly distribute the pressure points, the lower part is supposed to represent the inner lower part of the shoe. Podiatrists take into account the first condition by molding the feet, but not the second condition. The insole creation is not as easy as one can imagine. Different parameters and technical criteria are involved in the creation process [20]. A sole must also cushion shocks when you put your foot on the ground, stabilize and align the body in its natural position, or even compensate for differences in leg length. Bad insoles can cause fatigue in the feet, legs or create musculoskeletal disorders. A bad fit of the foot in the shoe does not optimize the unwinding of walking.

Depending on the needs of use (the city, running, hiking, the type of sport ..) or pathology that has been detected by the podiatrist, the role of the insole can be different and the designers of insoles act on the cushioning by gel, on the thickness, on the posture and hygiene, on its lightness and its dynamism, its protection, its insulating power [21]. This product can then be designed in different natural or synthetic materials, multi-material with zoning. It is a very technical element very often using the distribution of the pressure during a medical analysis.

Matter is very important, but good fit foot into the shoe with specific insole is also very important. Also, this work is oriented on the implementation of a process of creation of insole adapted to the patient's morphology. This process is in 3D to follow the feet morphology and the inside shoe morphology represented by a shoe-last respecting the industrial size of the patient.

2. Wedging system of the foot

In the case of a manual measurement, the heel must be wedged on a first plane and the inner side of the foot on another plane perpendicular to that of the heel. In an automatic process developed in CAD system, these

operations can be carried out using planes perpendicular to the ground. The difference with the manual process is that we have to wedge in first the inner side of the foot on its plane before wedging the heel on its own plane. This procedure has to need different tracking techniques of anthropometric points through the use of different adjustable planes.

For the plane of the inner side, we use a search technique using two contact points A and B to wedge the plane containing these points on the inner side of the foot (Figure 1). This shift is performed relative to the original marker of the scanner (OriginReference). The line Ox, supporting the starting plane and designed in a new reference frame R1, can move along the Y axis and then turn towards around the Z-axis. The two contact zones are detected by consecutively performing different translations and rotations in an alternative manner with a dichotomy approach. The quality of the contact is reached by gradually refining the translation and rotation parameters value.

For the plane of the heel, another search technique using uniquely one point of contact C is used by wedging the heel on the plane perpendicular to the previous plane (Figure 1). A line Oy supporting this plane, created in a new reference frame R2, can move perpendicularly to the line Ox as it is directly controlled from the reference frame R1. By a dichotomy approach, the contact zone can thus be detected with accuracy.

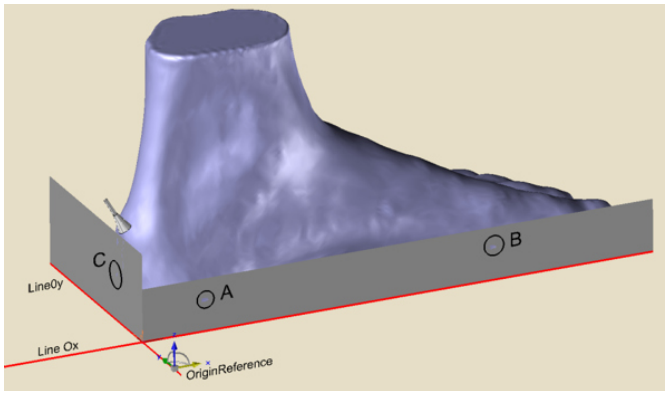

Figure 1: Contact points detection by plane techniques.

This first step was to position the foot with respect to a new 3D Cartesian coordinates integrating the reference frames R1/R2 which are none other than the footing blocking reference frames.

3. Plantar surface model

The 3D method used to construct the plantar surface is close to the 2D graphical method proposed by Rigal [20]. The interest of his graphical method is to connect various technical data used to design the shoe-last representing the interface between the shoe style and the anatomical information of the foot. For various reasons, the shoe-last, the shoe, the foot and the insole have to be connected in the same design process. For example, the design, shape and volume of the shoe last are crucial for the fit of a shoe. The insole design whose upper form represents the lower part of the foot, have to be connected to the inside part of the shoe i.e. the lower shape of the shoe-last.

This 3D shape association has led us to a plantar surface design process in relation with the shoe-last which passes through four distinct steps which will be described hereinafter.

3.1. Geometry plot of optimal outline encompassing the footprint

In a first phase, we followed carefully the Rigal's method by adjusting only the dimensional characteristics obtained by the foot scan, ie:

- length of the foot (280.6 mm)
- perimeter of ball girth (278.7)
- perimeter of instep girth (282.1)
- length between heel to 5th toe (234)

For this foot size, others parameters have been chosen in the size chart of the database coming from the feet statistical analysis of the French population [20]. The author does not specify the date and the protocol of the measurement campaign, the unique information that has been given is that the statistical analysis has been realized with a men and women sample of 10000.

The data extracted of the size chart are essentially the angle measurements of the footprint, ie:

- metatarsophalangeal ball angle OCC' (71°06)
- 1st toe angle ACR' (13°94)
- 5th toe angle S'C'Q' (10°22)

The graphical method to trace outline encompassing the footprint follows the procedure described in the Figure 2

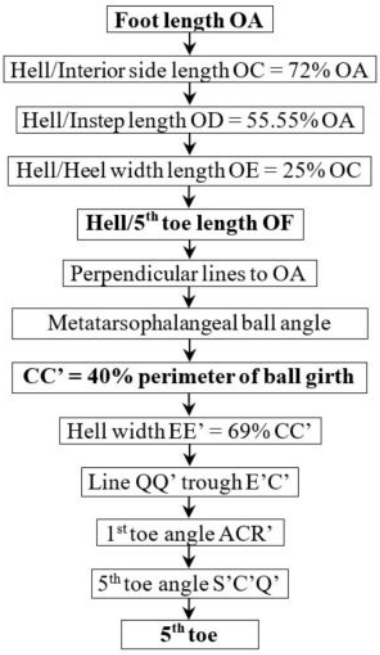

Figure 2: Outline encompassing the footprint drawing procedure.

Figure 3 shows that the foot is not completely inscribed in the contour formed by the points OCR'S'C'Q.

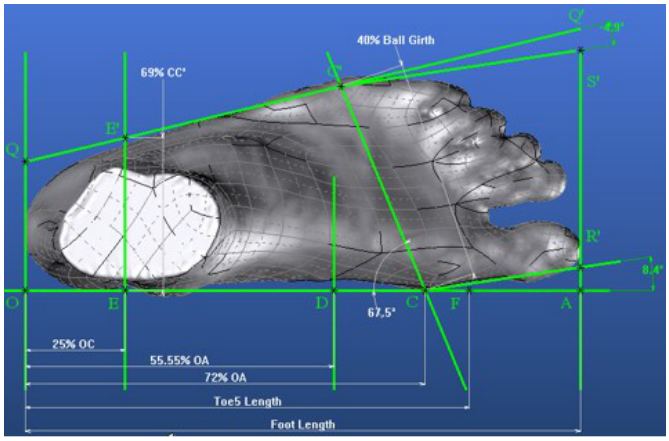

Figure 3: Rigal's method to draw outline encompassing the footprint.

This gap was foreseeable as this procedure is applicable only to average data from the statistical analysis of the foot measurement campaign. By observing this result, it can be seen that a better detection of the contact zones and an adjustment of the different angles could lead to better results.These two problems can be solved by our contact point's detection techniques by parametric plane (Figure 4).

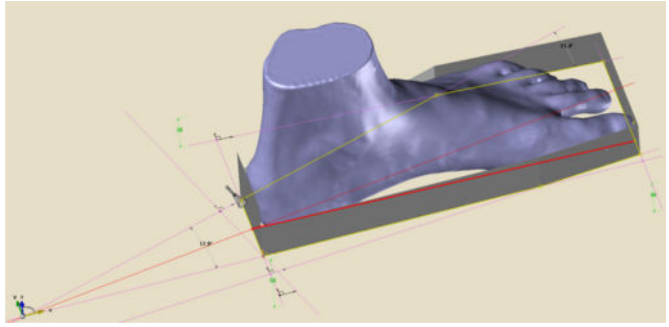

Figure 4: Contact points Method to define the optimal outline encompassing the footprint.

Thus, the line QQ' can be adjusted by a plane at two contacts (**Figure 3**). The two angles ACR ', S'C'Q' can then be adjusted by a plane at one contact pivoting respectively in C and C'.

The position of the pivot points C and C' are the two contact points resulting from the preceding search; the point C giving the position of the metatarsal tibiae, the point C' the position of the metatarsal fibular.

The results of the **Figure 5** show that the foot is perfectly inscribed in the new outline encompassing the footprint. The difference with the Rigal's method is that many parameters have been obtained automatically by a direct measurement and these parameters no longer control the shape of this new boundary.

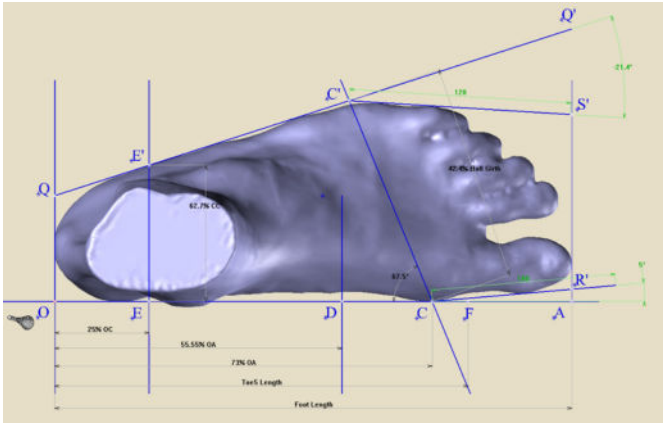

Figure 5 : Optimal outline encompassing the footprint**.**

The new values of these measurement data are:

OC = 73% OA, CC '= 42.4% Ball girth, EE' = 62.7% CC ', Angle ACR' = 5 °, Angle OCC '= 67.5 °, Angle S'C'Q' = 21.4 °.

The foot length can also be detected by a plane R 'S' perpendicular to the line OA and tangent on the extremity of the 1st toe. The new value OA defining the foot length is 280.2 mm which represents a French size close to 44. The conversion of the foot length to the French size (abacus from [20]) is given by the following equation:

*Shoe size = 0.1602 * FootLenght - 0.6607*

3.2. Connection between outline encompassing the footprint and the shoe-last

At this stage of the study, we can choose the good shoe last according to the shoe size in order to know the inner shape of the shoe. Table 1 gives us the evolution of the numbered shoe-last according to the shoe size. For example, if we take a shoe last of 6th for a shoe size of 44, the finger perimeter of the shoe-last will take the value 250. This finger perimeter and the ball girth perimeter of the foot are connected by a value of ease allowance. For a better foot support in the shoe and increase comfort, the shoe last has to be longer and narrower than the foot. His length and volume depend on the type of shoe. For example, for a sandal, we have to increase the length of 2%, of 3% for square toe, 4% for round toe and so on. In our case, the number of the shoe last is 8th (ball girth perimeter = 277.4, finger perimeter = 260).

Table 1: "Point de PARIS" of the shoe-last according to the shoe size.

Shoe size	Width							
"Point de PARIS"	1st	2nd	3rd	4th	5th	6th	7th	8th
33	170	175	180	185	190	195	200	205
34	175	180	185	190	195	200	205	210
35	180	185	190	195	200	205	210	215
36	185	190	195	200	205	210	215	220
37	190	195	200	205	210	215	220	225
38	195	200	205	210	215	220	225	230
39	200	205	210	215	220	225	230	235
40	205	210	215	220	225	230	235	240
41	210	215	220	225	230	235	240	245
42	215	220	225	230	235	240	245	250
43	220	225	230	235	240	245	250	255
44	225	230	235	240	245	250	255	260
45	230	235	240	245	250	255	260	265
46	235	240	245	250	255	260	265	270
47	240	245	250	255	260	265	270	275
48	245	250	255	260	265	270	275	280

The graphical method to trace the lines connecting the outline encompassing the footprint and the shoe-last follows the procedure described in the Figure 6.

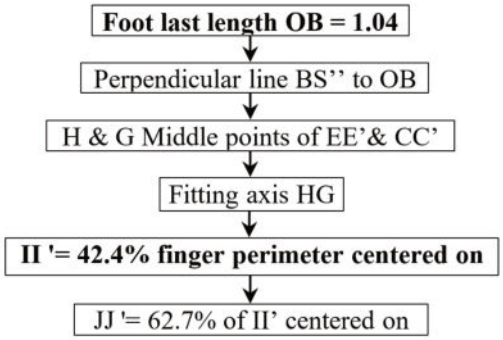

Figure 6: Outline encompassing the footprint drawing procedure.

The procedure shows that the shoe last length is proportional to the foot length (increasing of 4% due to the round toe). The fitting axis is given by the direction of the line passing through the midpoints H of EE' and G of CC'. These red lines represent the projection of the outline encompassing the shoe-last (Figure 7).

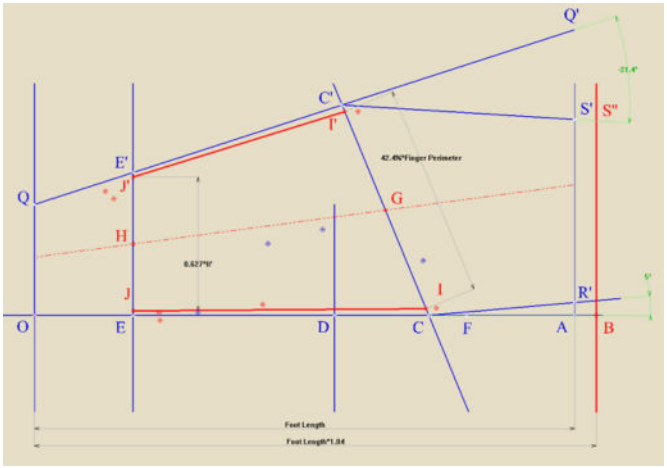

Figure 7: Projection of the outline encompassing the shoe last.

3.3. Characteristic points identification of plantar surface of shoe-last

The graphical method to locate the position of the characteristic points of the plantar surface follows the procedure described in the Figure 8.

The first step consists in positioning the points LL' distributed at an equal distance from the point G defining the plantar surface width (**Figure 9**). Then, we have to locate the narrowest part of the foot arch. His position is defined with respect to a point situated on the axis OA, proportional to the length of the foot. U represents the projection perpendicular of this point on the fitting axis HG.

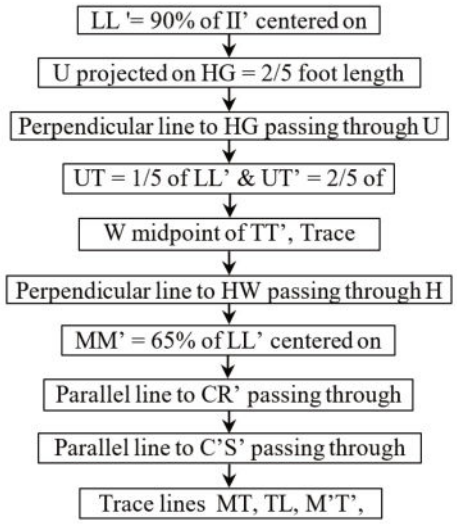

Figure 8: Locating the position of the characteristic points of the plantar surface of the shoe last

On a line perpendicular to the fitting axis passing through U, two points T and T' are located to define the width of the narrowest part of the foot arch. The midpoint W of the points T, T' and the point H make it possible to trace the symmetry axis of the heel. On a line perpendicular to the symmetry axis of the heel passing through H, two points J and J' are located to define the heel width. The heel extremity is generated by a circle of diameter MM' whose center can slide on the symmetry axis of the heel in order to control the distance between this circle and the axis OQ. This distance is conditioned by the shape of the rear curve of the shoe last. The extremity point of the plantar surface end is tangent to BS''.

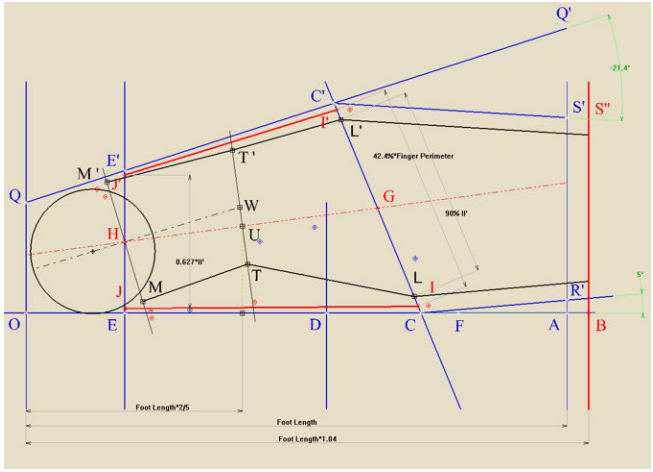

Figure 9: Characteristic points of the plantar surface of the shoe last.

3.4. Outline of plantar surface contour

The follow-up of this plot gives us a curve representing the plantar surface (Figure 10: red curve).

If we compare the plantar surface with the foot, we notice that the curve perfectly follows the contour of the foot with a decreased ratio conforming to the design of a shoe-last (Figure 11a). The pressure of the foot on the scanner glass also gives a good match with the plantar surface (Figure 11b).

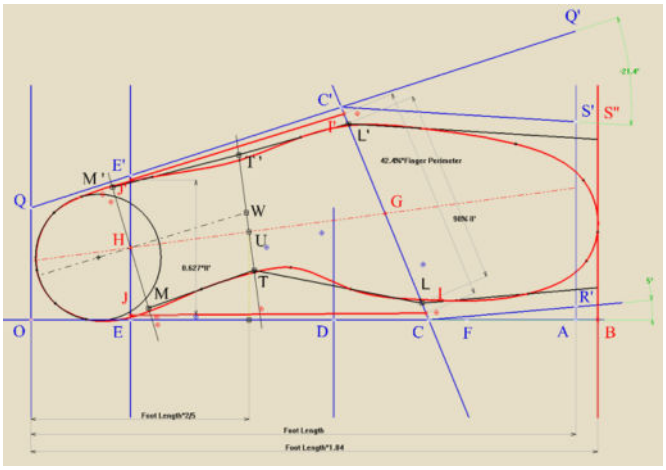

Figure 10: Drawing the outline of plantar surface contour.

If we compare the plantar surface with the foot, we notice that the curve perfectly follows the contour of the foot with a decreased ratio conforming to the design of a shoe-last (Figure 11a). The pressure of the foot on the scanner glass also gives a good match with the plantar surface (Figure 11b).

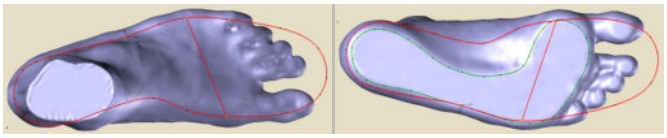

Figure 11: Matching between the foot and the outline of plantar surface contour.

4. Analysis between foot and shoe-last

In a first analysis, it can be interresting to compare the foot with the shoe-last choosen in the good range of size. Figure 12a shows that the two shape are quite close. We only notice that the edge to the fingers corresponding to the 6th width of a shape is not verified because the shape is given for a width.

In this case, it is necessary to adjust the shoe-last to take into account the width of the foot larger. A homothety of ratio 1.076 on the shoe-last with ball girth value of 250mm was carried out in order to obtain the good ball girth value of 269mm (Figure 12b). We can consider that the number of the shoe-last is 9th, beyond the limit of Table 1.

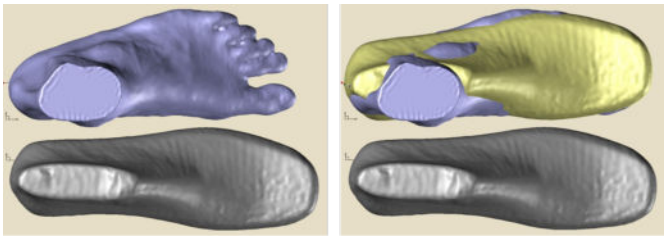

Figure 12: Adjustment of the shoe-last.

This adjustment of the shoe-last makes it possible to check if the insole which has been adapted to the foot morphology correctly follows the shoe-last one which represents the inner part of the shoe. Figure 13 shows that the front part of the plantar surface perfectly follows the shoe-last morphology. But the back part has an offset at the heel which will be necessary to take into account by slightly reorienting this area by the inclination of the axis TWT' (Figure 10). This adjustment will be made later on the lower part of the sole when it is created in 3D.

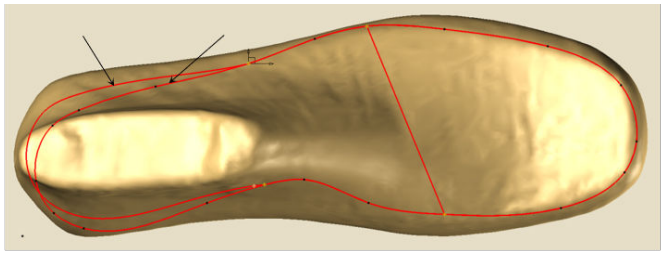

Figure 13: Plantar surface difference between foot and shoe-last ajusted.

5. 3D insole model

The knowledge of the plantar surface is important because it represents the strategic outline to represent the 3D shape of the insole. At this stage of the design process, we need to look for the contact areas between the foot and the shoe-last in order to create an insole morphologically fitted to the patient's foot. This creation must take into account the previous constraints by using the two plantar surfaces: plantar surface of the foot, plantar surface of the shoe-last.

5.1. 3D below surface of insole

The below of the insole should represent the contact area with the boot, ie the bottom surface of the shoe-last. The 2D contour is represented by the plantar surface of shoe-last in **Figure 13.** A printing of this 2D contour was first made on the shoe-last to obtain its 3D representation connected to the shoe-last (**Figure 14a**). Then, the mesh of the internal surface of this printed contour (**Figure 14a**) was made in order to create a 3D surface representing the bottom surface of the insole (**Figure 14b.c**).

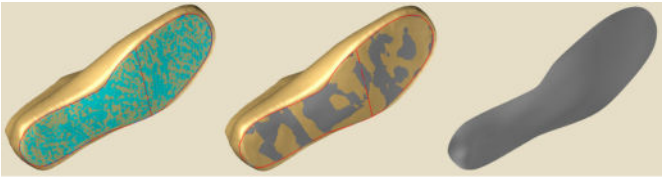

Figure 14: Creation process of the insole below surface.

5.2. 3D above surface of insole

The above of the insole should represent the foot contact area, ie the bottom surface of the foot. The 2D contour is represented by the plantar surface of the foot in **Figure 13**. This contour was separated into two parts cut by the line of ball girth (**Figure 15a**). Two printings of this 2D line were made: one on the back part of the foot, the other on the front part of the shoe-last (forepart). We printed on the front part to take into account the value of the toe spring measurement of the forepart, according to the 3D shoe-last shape. In addition, the forepart of the shoe-last does not present the misalignment of the backpart.

Then, the mesh of each inner surface of these printed contours (**Figure 15b**) was made to create two 3D surfaces. These surfaces were sewn to obtain the upper surface of the insole (**Figure 15c, Figure 15a**).

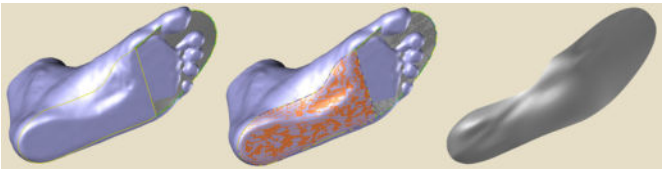

Figure 15: Creation process of the insole above surface.

5.3 3D insole

On the contours of the above and below surfaces of the insole (Figure 16a) is created a peripheral surface to create a closed continuous surface (Figure 16b.c). These three surfaces are then sewn to obtain the final surface of the 3D insole (Figure 16d).

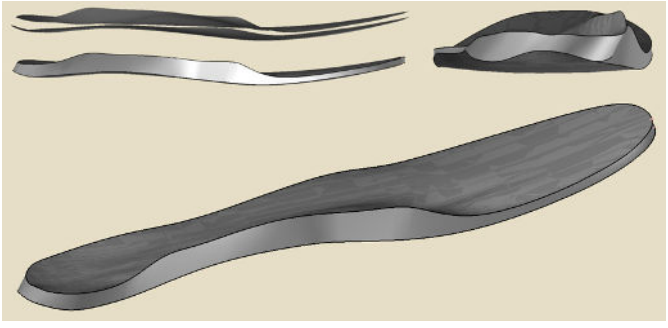

Figure 16: Création process of 3D insole surface.

6. Conclusion

This study was carried out with a shoe-last standard in order to respect the existing standards of the footwear industry. The analysis of the interface between the shoe-last and the adjusted insole showed a significant difference between the morphology of the shoe-last standard and the foot whose morphology was taken at random from our database. This gap forced us to adjust the underside of the footing showing an unbalanced 3D deformation (Figure 16c). This phenomenon can in some cases lead to a lack of comfort if this adjustment is too high. Also, future work has been focused on the implementation of shoe-last adapted to the feet morphology in order to perfectly adjust this inseparable block represented by the foot, the insole and the shoe-last.

7. References

[1] T. Duckworth, R. P. Betts, C. I. Franks, and J. Burke, “The Measurement of Pressures under the Foot,” *Foot Ankle Int.*, vol. 3, no. 3, pp. 130–141, 1982.

[2] D. Rosenbaum and H.-P. Becker, “Plantar pressure distribution measurements. Technical background and clinical applications,” *Foot Ankle Surg.*, vol. 3, no. 1, pp. 1–14, Jan. 1997.

[3] L. Mateu and F. Moll, “Optimum piezoelectric bending beam structures for energy harvesting using shoe inserts,” *J. Intell. Mater. Syst. Struct.*, vol. 16, no. 10, pp. 835–845, 2005.

[4] J. Zhao and Z. You, “A shoe-embedded piezoelectric energy harvester for wearable sensors,” *Sensors (Switzerland)*, vol. 14, no. 7, pp. 12497–12510, 2014.

[5] A Almusallam et al, “Screen-printed piezoelectric shoe-insole energy harvester using an improved flexible PZT-polymer composites Screen-printed piezoelectric shoe-insole energy harvester using an improved flexible PZT-polymer composites,” in *Journal of Physics*, 2013.

[6] J. Zhao, Y. Guo, and L. Wang, “An Insole Plantar Pressure Measurement System Based on 3D Forces Piezoelectric Sensor,” *Sensors & Transducers*, vol. 160, no. 12, pp. 49–54, 2013.

[7] M. Tenten-Diepenmaat *et al.*, “In-shoe plantar pressure measurements for the evaluation and adaptation of foot orthoses in patients with rheumatoid arthritis: A proof of concept study,” *Gait Posture*, vol. 45, pp. 45–50, 2016.

[8] J. Perttunen, *Foot loading in normal and pathological walking*. 2002.

[9] T. F. Novacheck, “Review Paper The biomechanics of running,” *Gait Posture*, vol. 7, pp. 77–95, 1998.

[10] K. G. Prabhu, D. Agrawal, K. M. Patil, and S. Srinivasan, “Parameters for analysis of walking foot pressures at different levels of diabetic neuropathy and detection of plantar ulcers at early stages,” *Itbm-Rbm*, vol. 22, no. 3, pp. 159–169, 2001.

[11] N. L. W. Keijsers, N. M. Stolwijk, J. W. K. Louwerens, and J. Duysens, “Classification of forefoot pain based on plantar pressure measurements,” *Clin. Biomech.*, vol. 28, no. 3, pp. 350–356, 2013.

[12] A. Paiva de Castro, J. R. Rebelatto, and T. R. Aurichio, “The relationship between foot pain, anthropometric variables and footwear among older people,” *Appl. Ergon.*, vol. 41, no. 1, pp. 93–97, 2010.

[13] S. K. van de Velde, M. Cashin, R. Johari, R. Blackshaw, A. Khot, and H. K. Graham, “Symptomatic hallux valgus and dorsal bunion in adolescents with cerebral palsy: clinical and biomechanical factors,” *Dev. Med. Child Neurol.*, vol. 60, no. 6, pp. 624–628, 2018.

[14] D. M. Aaron, “Pied d’athlčte (tinea pedis),” *Le Manuel MSD*, 2016. [Online]. Available: https://www.msdmanuals.com/fr/accueil/troubles-cutanés/infections-mycosiques-de-la-peau/pied-d’athlčte-tinea-pedis.

[15] “Boite ŕ empreintes double - Salembier Pédicurie Podologie.” [Online]. Available: http://salembier.fr/boites-a-empreintes-et-moulage/1146-boite-a-empreintes-double.html. [Accessed: 20-Aug-2019].

[16] R. C. C. Chen, “An investigation into shoe last design in relation to foot measurement and shoe fitting for orthopaedic footwear,” London, 1993.

[17] C. P. Witana, S. Xiong, J. Zhao, and R. S. Goonetilleke, “Foot measurements from three-dimensional scans: A comparison and evaluation of different methods,” *Int. J. Ind. Ergon.*, vol. 36, no. 9, pp. 789–807, 2006.

[18] B. Sarghie, M. Costea, and D. Liute, “Anthropometric Study of the Foot Using 3D Scanning Method and Statistical Analysis,” *Int. Symp. Knitt. Appar.*, no. May, pp. 1–5, 2013.

[19] “BFTS GmbH.” [Online]. Available: https://www.bfts.de/. [Accessed: 19-Aug-2019].

[20] R. RIGAL and D. MOTTIN, *La forme*, Lyon, CTC. 1991.

[21] M. Mandolini, A. Brunzini, and M. Germani, “A collaborative web-based platform for the prescription of Custom-Made Insoles,” *Adv. Eng. Informatics*, vol. 33, pp. 360–373, 2017.